Available online at www.sciencedirect.com
ScienceDirect
Trans. Nonferrous Met. Soc. China 24(2014) 1547−1553
Transactions of Nonferrous Metals Society of China
www.tnmsc.cn

Modified algorithm of combined GPS/GLONASS precise point positioning for applications in open-pit mines

Chang-sheng CAI, Xiao-min LUO, Jian-jun ZHU

School of Geosciences and Info-Physics, Central South University, Changsha 410083, China

Received 10 July 2013; accepted 17 January 2014

Abstract: A modified algorithm of combined GPS/GLONASS precise point positioning (GG-PPP) was developed by decreasing the number of unknowns to be estimated so that accurate position solutions can be achieved in the case of less number of visible satellites. The system time difference between GPS and GLONASS (STDGG) and zenith tropospheric delay (ZTD) values were firstly estimated in an open sky condition using the traditional GG-PPP algorithm. Then, they were used as a priori known values in the modified algorithm instead of estimating them as unknowns. The proposed algorithm was tested using observations collected at BJFS station in a simulated open-pit mine environment. The results show that the position filter converges much faster to a stable value in all three coordinate components using the modified algorithm than using the traditional algorithm. The modified algorithm achieves higher positioning accuracy as well. The accuracy improvement in the horizontal direction and vertical direction reaches 69% and 95% at a satellite elevation mask angle of 50°, respectively.

Key words: GPS; GLONASS; precise point positioning; elevation mask angle; open-pit mine

1 Introduction

Precise point positioning (PPP) is a technique that uses dual-frequency carrier phase observations from a single receiver along with precise satellite orbit and clock products to achieve an accuracy of decimeter to centimeter level [1,2]. In the past, the PPP technique was mainly implemented using GPS-only observations. But for such a satellite-based positioning technique, the accuracy, availability and reliability of position solutions are largely dependent on the number of visible satellites. In open-pit mines, the number of tracked GPS satellites is often insufficient to obtain a high-accuracy positioning solution. With the revitalization and modernization of GLONASS [3], the combined use of GPS and GLONASS has attracted increasing interest in the GNSS (Global Navigation Satellite Systems) community. In recent years, some researchers investigated the combined GPS/GLONASS PPP (GG-PPP) approaches [4−9] and the results have indicated improved performance over GPS-only PPP especially in the environment with limited satellite visibility [7].

In the traditional GG-PPP observation model, the estimated unknown parameters include three coordinate components, one receiver clock offset, one system time difference between GPS and GLONASS (STDGG), one zenith tropospheric delay (ZTD), and ambiguities equal to a number of observed GPS and GLONASS satellites [4]. It is apparent that there are too many unknown parameters that need to be solved. The more the number of the unknowns is, the more the required number of visible satellites is. Although the integration of GPS and GLONASS almost doubles the number of visible satellites, the observed satellites could still be insufficient in open-pit mines due to too many unknowns to be estimated and less number of visible satellites. In order to enable the PPP applications in such a situation, an effective strategy is to reduce the number of the unknowns in the GG-PPP approach.

A modified GG-PPP algorithm is proposed by removing the unknown parameters of the STDGG and ZTD from the observation model. Instead of estimating the two unknowns, their values are determined in advance in an open sky condition using the traditional algorithm. The performance of the traditional GG-PPP

Foundation item: Project (41004011) supported by the National Natural Science Foundation of China; Project (2014M550425) supported by the China Postdoctoral Science Foundation
Corresponding author: Chang-sheng CAI; E-mail: cscai@hotmail.com
DOI: 10.1016/S1003-6326(14)63224-6

algorithm is first assessed by comparing with GPS-only PPP using real observations but in a simulated open-pit mine environment. The modified GG-PPP algorithm is then tested and the results are compared with those obtained from the traditional algorithm.

2 Combined GPS/GLONASS PPP algorithm

2.1 Traditional algorithm

For a dual-frequency GPS/GLONASS receiver, the pseudorange and carrier phase observations on L_1 and L_2 frequencies between a receiver and a satellite can be written as [4]

$$P_i^{\mathrm{g}} = \rho^{\mathrm{g}} + c\Delta t - c\Delta T^{\mathrm{g}} + d_{\mathrm{orb}}^{\mathrm{g}} + m^{\mathrm{g}} d_{\mathrm{trop}}^{\mathrm{g}} + d_{\mathrm{ion}/L_i}^{\mathrm{g}} + d_{\mathrm{mult}/P_i}^{\mathrm{g}} + \varepsilon_{P_i}^{\mathrm{g}} \tag{1}$$

$$\Phi_i^{\mathrm{g}} = \rho^{\mathrm{g}} + c\Delta t - c\Delta T^{\mathrm{g}} + d_{\mathrm{orb}}^{\mathrm{g}} + m^{\mathrm{g}} d_{\mathrm{trop}}^{\mathrm{g}} - d_{\mathrm{ion}/L_i}^{\mathrm{g}} + \lambda_i N_i^{\mathrm{g}} + d_{\mathrm{mult}/\Phi_i}^{\mathrm{g}} + \varepsilon_{\Phi_i}^{\mathrm{g}} \tag{2}$$

$$P_i^{\mathrm{r}} = \rho^{\mathrm{r}} + c\Delta t + c\Delta t_{\mathrm{sys}} - c\Delta T^{\mathrm{r}} + d_{\mathrm{orb}}^{\mathrm{r}} + m^{\mathrm{r}} d_{\mathrm{trop}}^{\mathrm{r}} + d_{\mathrm{ion}/L_i}^{\mathrm{r}} + d_{\mathrm{mult}/P_i}^{\mathrm{r}} + \varepsilon_{P_i}^{\mathrm{r}} \tag{3}$$

$$\Phi_i^{\mathrm{r}} = \rho^{\mathrm{r}} + c\Delta t + c\Delta t_{\mathrm{sys}} - c\Delta T^{\mathrm{r}} + d_{\mathrm{orb}}^{\mathrm{r}} + m^{\mathrm{r}} d_{\mathrm{trop}}^{\mathrm{r}} - d_{\mathrm{ion}/L_i}^{\mathrm{r}} + \lambda_i^{\mathrm{r}} N_i^{\mathrm{r}} + d_{\mathrm{mult}/\Phi_i}^{\mathrm{r}} + \varepsilon_{\Phi_i}^{\mathrm{r}} \tag{4}$$

where the superscripts “g” and “r” denote a GPS satellite and a GLONASS satellite, respectively; P_i is the measured pseudorange on L_i, m; Φ_i is the measured carrier phase on L_i, m; ρ is the geometric range, m; c is the speed of light, m/s; Δt is the receiver clock offset, s; Δt_{sys} is the system time difference between GPS and GLONASS, s; ΔT is the satellite clock offset, s; d_{orb} is the satellite orbit error, m; d_{trop} is the zenith tropospheric delay, m; m is the mapping function; d_{ion/L_i} is the ionospheric delay on L_i, m; λ_i is the GPS carrier wavelength on L_i, m; λ_i^{r} is the carrier wavelength on L_i for a GLONASS satellite “r”, m; N_i is the phase ambiguity term on L_i in cycles; d_{mult/P_i} and d_{mult/Φ_i} are the multipath effect in the measured pseudorange and carrier phase on L_i, m, respectively; ε is the measurement noise, m.

After applying the precise satellite orbit and clock corrections as well as other error corrections that need to be considered in PPP [2], the ionosphere-free code and carrier phase observables for GPS and GLONASS can be expressed as

$$P_{\mathrm{IF}}^{\mathrm{g}} = \rho^{\mathrm{g}} + c\Delta t + m^{\mathrm{g}} d_{\mathrm{trop}}^{\mathrm{g}} + \varepsilon_{P_{\mathrm{IF}}}^{\mathrm{g}} \tag{5}$$

$$\Phi_{\mathrm{IF}}^{\mathrm{g}} = \rho^{\mathrm{g}} + c\Delta t + m^{\mathrm{g}} d_{\mathrm{trop}}^{\mathrm{g}} + N_{\mathrm{IF}}^{\mathrm{g}} + \varepsilon_{\Phi_{\mathrm{IF}}}^{\mathrm{g}} \tag{6}$$

$$P_{\mathrm{IF}}^{\mathrm{r}} = \rho^{\mathrm{r}} + c\Delta t + c\Delta t_{\mathrm{sys}} + m^{\mathrm{r}} d_{\mathrm{trop}}^{\mathrm{r}} + \varepsilon_{P_{\mathrm{IF}}}^{\mathrm{r}} \tag{7}$$

$$\Phi_{\mathrm{IF}}^{\mathrm{r}} = \rho^{\mathrm{r}} + c\Delta t + c\Delta t_{\mathrm{sys}} + m^{\mathrm{r}} d_{\mathrm{trop}}^{\mathrm{r}} + N_{\mathrm{IF}}^{\mathrm{r}} + \varepsilon_{\Phi_{\mathrm{IF}}}^{\mathrm{r}} \tag{8}$$

where P_{IF} is the corrected ionosphere-free code observable, m; Φ_{IF} is the corrected ionosphere-free phase observable, m; N_{IF} is the ionosphere-free ambiguity term, m; $\varepsilon_{P_{\mathrm{IF}}}$ and $\varepsilon_{\Phi_{\mathrm{IF}}}$ contain measurement noise, multipath as well as other residual errors, m. The unknown parameters in the observation model include three coordinate components, one receiver clock offset, one STDGG, one ZTD and ambiguities. The receiver clock offsets are usually modeled as random walk (RW) or first-order Gauss−Markov processes [10,11]. The STDGG and ZTD can be modeled as RW processes [12], while the ambiguity parameters and static position coordinates are considered constants.

2.2 Modified algorithm

In the modified GG-PPP algorithm, the STDGG and ZTD are removed from the unknown parameters to be estimated. Instead of solving them as unknowns, their a priori known values that are obtained using the traditional algorithm under an open sky observing condition are applied to correctting observations based on the fact that the STDGG and ZTD remain stable over a short period of time. After removing the unknowns of the STDGG and ZTD, the observation model in the modified algorithm is simplified as

$$P_{\mathrm{IF}}^{\prime\mathrm{g}} = \rho^{\mathrm{g}} + c\Delta t + \varepsilon_{P'_{\mathrm{IF}}}^{\mathrm{g}} \tag{9}$$

$$\Phi_{\mathrm{IF}}^{\prime\mathrm{g}} = \rho^{\mathrm{g}} + c\Delta t + N_{\mathrm{IF}}^{\mathrm{g}} + \varepsilon_{\Phi'_{\mathrm{IF}}}^{\mathrm{r}} \tag{10}$$

$$P_{\mathrm{IF}}^{\prime\mathrm{r}} = \rho^{\mathrm{r}} + c\Delta t + \varepsilon_{P'_{\mathrm{IF}}}^{\mathrm{r}} \tag{11}$$

$$\Phi_{\mathrm{IF}}^{\prime\mathrm{r}} = \rho^{\mathrm{r}} + c\Delta t + N_{\mathrm{IF}}^{\mathrm{r}} + \varepsilon_{\Phi'_{\mathrm{IF}}}^{\mathrm{r}} \tag{12}$$

where $P_{\mathrm{IF}}^{\prime\mathrm{g}}$ and $\Phi_{\mathrm{IF}}^{\prime\mathrm{g}}$ are the updated ones after applying the a priori ZTD corrections to $P_{\mathrm{IF}}^{\mathrm{g}}$ and $\Phi_{\mathrm{IF}}^{\mathrm{g}}$, respectively; Similarly, $P_{\mathrm{IF}}^{\prime\mathrm{r}}$ and $\Phi_{\mathrm{IF}}^{\prime\mathrm{r}}$ are the updated ones after applying the a priori STDGG and ZTD corrections to $P_{\mathrm{IF}}^{\mathrm{r}}$ and $\Phi_{\mathrm{IF}}^{\mathrm{r}}$, respectively.

3 Test results and analysis

In this section, the GG-PPP solutions based on the traditional algorithm were first analyzed using mixed GPS/GLONASS observations. The open-pit mine environments were simulated by setting different satellite elevation mask angles. Next, the modified GG-PPP algorithm was tested and compared with the traditional algorithm.

The dataset collected at the BJFS station on July 25, 2012 was used for PPP processing. The BJFS station is equipped with a dual-frequency GNSS receiver that can receive both GPS and GLONASS signals. The dataset has a data sampling interval of 30 s. The final precise satellite orbit and 30s-interval clock offset products from IAC (Information-Analytical Center, Russia) were used to correct the satellite orbit and clock errors. In the Kalman filter estimation, the initial standard deviation (STD) values of GPS and GLONASS code observations were set to be 0.3 m and 0.6 m, respectively. The initial STD values of both GPS and GLONASS phase observations were set to be 2 mm. The spectral density values for the ZTD, the receiver clock offset and the STDGG parameters were empirically set to be 10^{-9} m^2/s, 10^5 m^2/s and 10^{-7} m^2/s [13], respectively. The antenna model "igs08.atx" was used for both satellite and receiver antenna phase center corrections [14]. The station coordinates from IGS were used as the "true" coordinates to calculate the positional errors in the east, north and up directions, respectively.

3.1 Improvement analysis of combined GPS/GLONASS PPP over GPS-only PPP

The dataset was processed using the traditional GG-PPP algorithm at different elevation mask angles with a comparison with GPS-only PPP. The satellite elevation mask angles were set to be 30°, 40° and 50° for the purpose of simulating an open-pit environment, respectively.

Figures 1 and 2 show the position errors, number of visible satellites and PDOP values for GPS-only PPP and GG-PPP at different elevation mask angles. The results indicate that the convergence time in the horizontal coordinate components has been reduced significantly by adding GLONASS to GPS. Table 1 provides the RMS statistical values of position errors within the last one hour for all three coordinate components. The RMS statistics reflect a converged positioning accuracy. It is noted that the accuracy improvements are significant in three coordinate components, especially for the elevation mask angle of 40°. Its improvement rates in the east, north and up directions reach 20%, 53% and 67%, respectively. This is because the less number of GPS satellites are visible at the higher elevation mask angle. Thus, the improvement on the satellite geometry is more significant after adding GLONASS. As a result, the positioning performance is improved at a larger degree. This clearly suggests that the integration of GPS and GLONASS can significantly benefit from the increased number of tracked satellites and improved satellite geometry under the limited visibility conditions. In this sense, the combined use of GPS and GLONASS is more desirable for applications in the open-pit mines.

In Figs. 1 and 2, PDOPs at some epochs are unavailable. This is because a minimum satellite number of 5 and 4 is required in the GG-PPP and GPS-only PPP processings, respectively. When the actual number of visible satellites is fewer than the required minimum number, the PDOPs as well as position coordinates will not be computed at these epochs. When the elevation mask angle is further set to 50°, the GPS-only positioning solutions are unavailable for more epochs due to insufficient satellites. Therefore, their processing results are not plotted and displayed here.

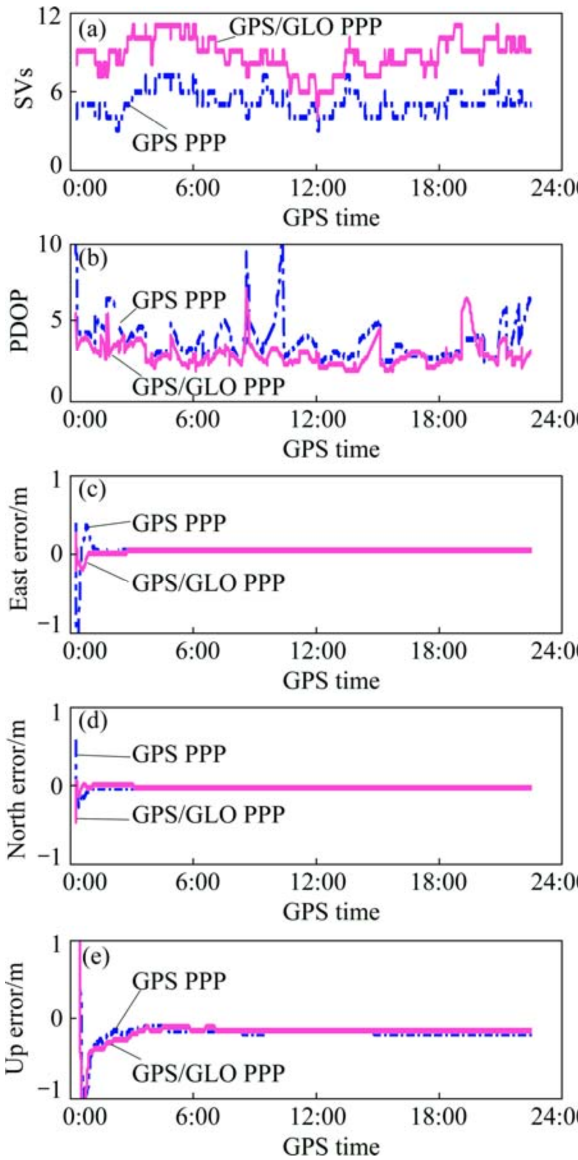

Fig. 1 GPS-only vs GPS/GLONASS positioning errors for PPP processings at elevation mask angle of 30°

Table 1 RMS statistics of position errors for GPS-only PPP and combined GPS/GLONASS PPP

Mask angle/(°)	System	Error/m		
		East	North	Up
30	GPS-only	0.046	0.028	0.203
	GPS/GLO	0.036	0.027	0.190
40	GPS-only	0.046	0.059	0.929
	GPS/GLO	0.037	0.028	0.306

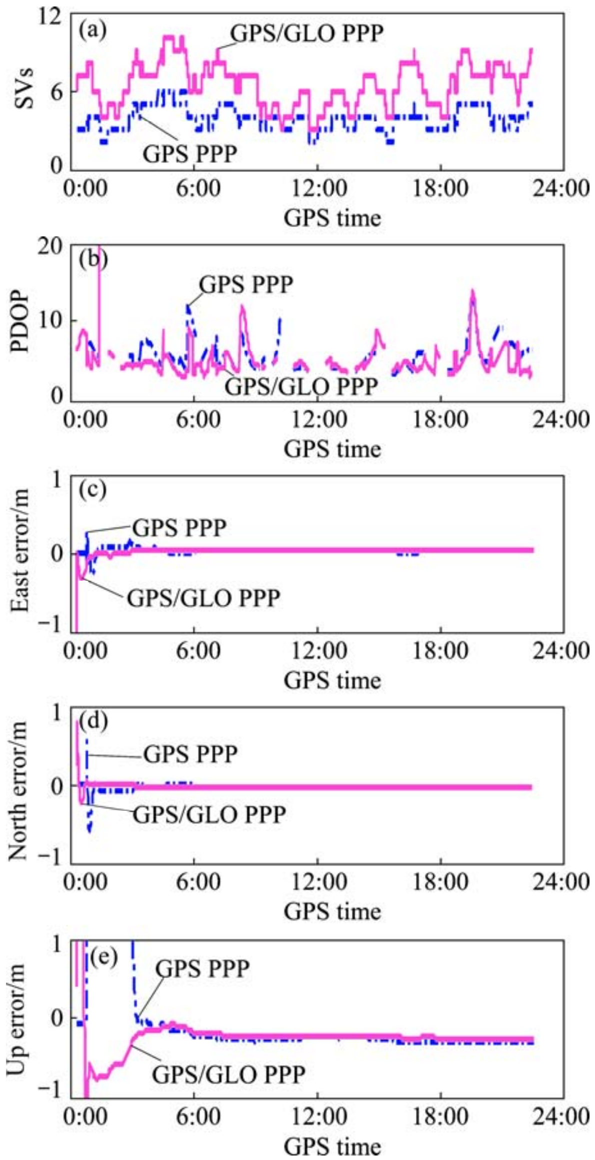

Fig. 2 GPS-only vs GPS/GLONASS positioning errors for PPP processing at elevation mask angle of 40°

3.2 Result analysis using modified algorithm

In order to test the performance of GG-PPP using the modified algorithm, the results are compared with the traditional algorithm.

Figure 3 shows the estimated epoch-by-epoch STDGG and ZTD values based on the traditional GG-PPP algorithm using the same dataset at an elevation mask angle of 10°. As can be seen, the STDGG and ZTD remain stable over one day. The large variations at the beginning are due to the convergence procedure of the position filter. The estimates of the STDGG vary in a range of 2 ns while the estimates of the ZTD values vary in a range of 10 cm after the position filter converges. More investigations regarding the time characteristics of the STDGG may refer to Ref. [15]. It is well known that the dry component of the ZTD is quite stable over short time. By contrast, its wet component is variable over time. But due to the fact that the wet component only accounts for 10%−20% of the ZTD, its variation is negligible using the modified algorithm.

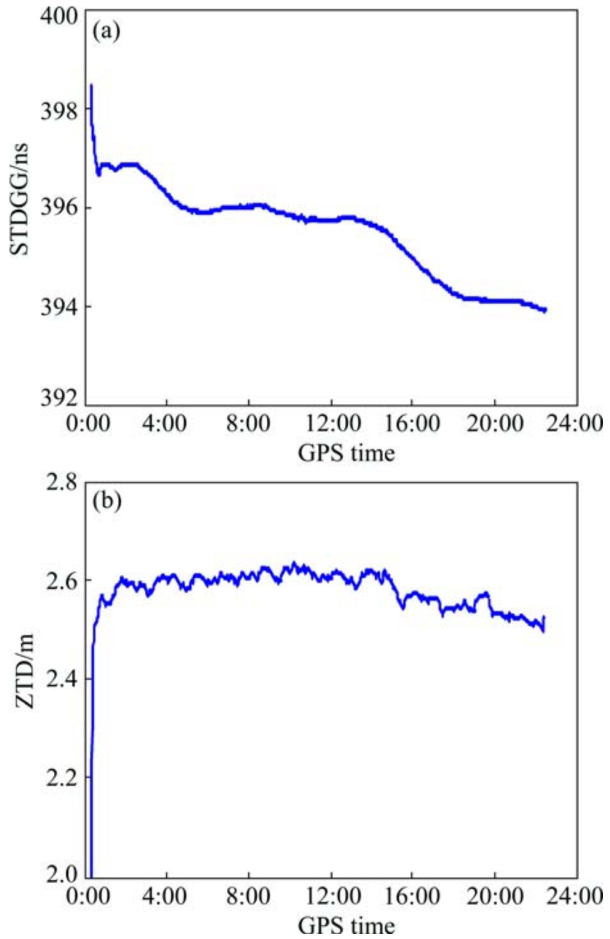

Fig. 3 Estimated system time difference values and zenith tropospheric delays at BJFS station

In the implementation of the modified algorithm, the traditional GG-PPP algorithm was firstly used to obtain estimates of the STDGG and ZTD in an open sky observing condition, as seen in Fig. 4. Figure 4 shows the epoch-by-epoch estimates of the STDGG and ZTD from GPS time 5:00 to 7:00 at an elevation mask angle of 10°. The estimated STDGG and ZTD values at the GPS time of 7:00 (i.e. the red cycles in Fig. 4) are then used as a priori known STDGG and ZWD values in the modified algorithm. With the a priori known STDGG and ZWD values, Figures 5−7 illustrate the GG-PPP processing results based on the modified algorithm using observations from 8:00 to 12:00 at elevation mask angles of 30°, 40° and 50°, respectively. The GG-PPP processing results using the traditional algorithm are also displayed for the purpose of comparison. It can be seen from these figures that the position filter converges much faster to a stable value in all three coordinate components

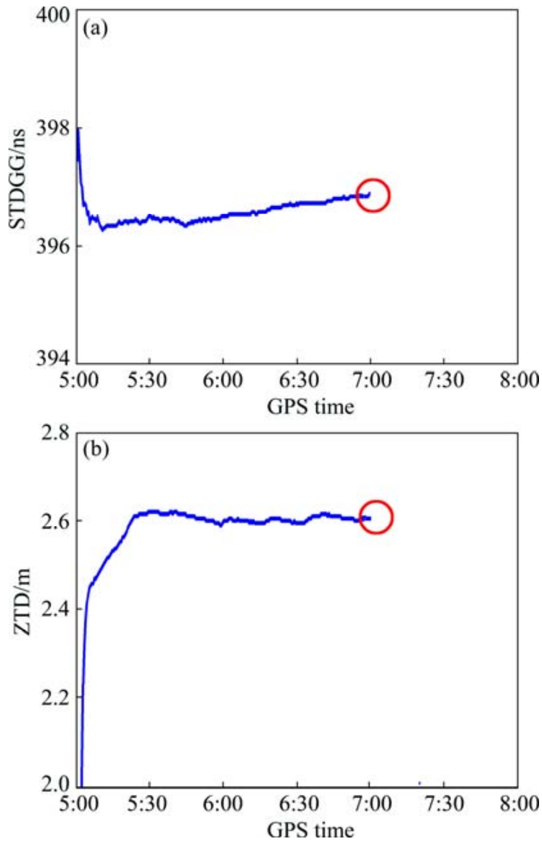

Fig. 4 Estimated STDGG (a) and ZTD (b) at BJFS station from GPS time 5:00 to 7:00

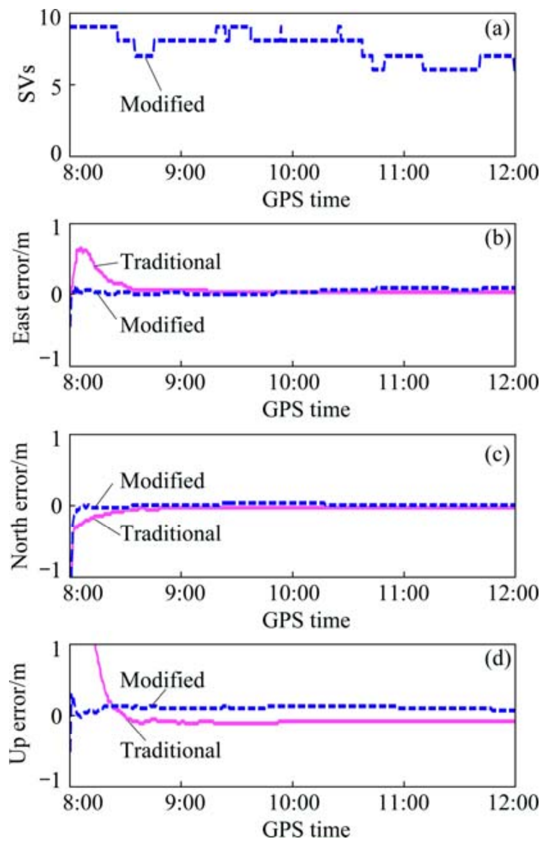

Fig. 5 Positioning errors for GG-PPP processing using traditional and modified algorithms at elevation mask angle of 30°

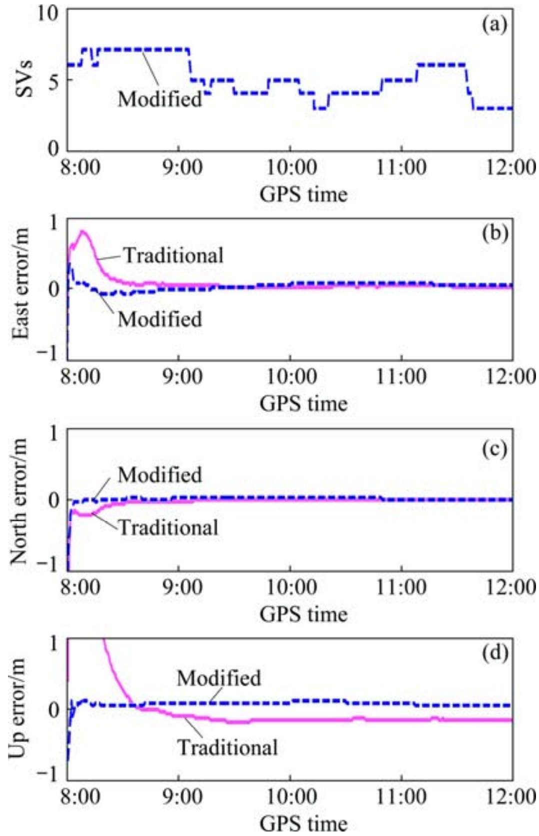

Fig. 6 Positioning errors for GG-PPP processing using traditional and modified algorithms at elevation mask angle of 40°

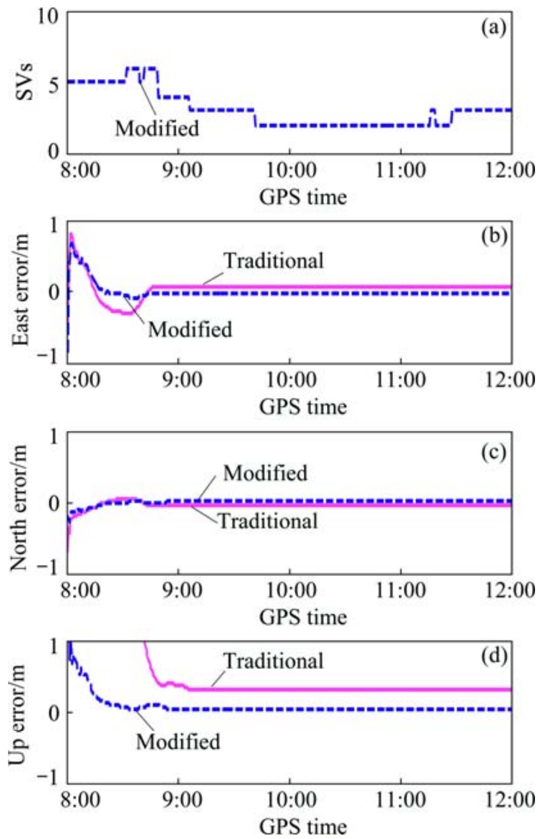

Fig. 7 Positioning errors for GG-PPP processing using traditional and modified algorithms at elevation mask angle of 50°

using the modified algorithm than the traditional algorithm.

Table 2 provides the RMS statistics of the last one-hour position errors. It is noted that the positioning accuracy degrades with the increase of the elevation mask angles from 30° to 50° using the traditional GG-PPP algorithm. However, it is not the case for the modified GG-PPP algorithm. Comparing their results using the two different algorithms, it is found that the modified algorithm achieves higher positioning accuracy, especially in the vertical component. The accuracy improvement is more significant under higher elevation mask angles. This means that reducing the unknown parameters indeed contributes to shortening the convergence time and improving the positioning accuracy in a limited satellite visibility environment.

Table 2 RMS values of position errors at different elevation mask angles

Mask angle/(°)	Algorithm	Error/m		
		East	North	Up
30	Traditional	0.030	0.022	0.098
	Modified	0.079	0.009	0.088
40	Traditional	0.030	0.023	0.163
	Modified	0.062	0.008	0.047
50	Traditional	0.051	0.046	0.317
	Modified	0.020	0.008	0.016

4 Conclusions

1) The combined GPS/GLONASS precise point positioning significantly improves positioning accuracy and reduces convergence time over GPS-only PPP in the simulated open-pit mine environment.

2) A modified algorithm was proposed by reducing two unknown parameters to be estimated, namely the system time difference between GPS and GLONASS (STDGG) and the zenith tropospheric delay (ZTD). Instead of estimating them as unknowns, their a priori known values that were obtained in the open-sky condition were used to correct observations.

3) The position solutions using the modified algorithm were compared with those acquired from the traditional GG-PPP algorithm. The results indicate that the modified algorithm can significantly improve the positioning accuracy as well as shorten the convergence time in the limited satellite visibility condition. The accuracy improvements in the horizontal direction and vertical direction reach 69% and 95% at a satellite elevation mask angle of 50°, respectively.

Acknowledgments

Contribution of data from IGS is greatly appreciated.

References

[1] ZUMBERGE J F, HEFLIN M B, JEFFERSON D C, WATKINS M M, WEBB F H. Precise point positioning for the efficient and robust analysis of GPS data from large networks [J]. Journal of Geophysical Research, 1997, 102 (B3): 5005−5017.

[2] KOUBA J, HEROUX P. Precise point positioning using IGS orbit and clock products [J]. GPS Solutions, 2001, 5(2): 12−28.

[3] URLICHICH Y, SUBBOTIN V, STUPAK G, DVORKIN V, POVALYAEV A, KARUTIN S. GLONASS modernization [C]//Proceedings of ION GNSS. Portland, Oregon, 2011: 3125−3128.

[4] CAI C, GAO Y. Performance analysis of precise point positioning based on combined GPS and GLONASS [C]//Proceedings of ION GNSS. Portland, Oregon, 2007: 858−865.

[5] HESSELBARTH A, WANNINGER L. Short-term stability of GNSS satellite clocks and its effects on precise point positioning [C]//Proceedings of ION GNSS. Savannah, Georgia, 2008: 1855−1863.

[6] MELGARD T, VIGEN E, JONG K D, LAPUCHA D, VISSER H, OERPEN O. G2—The first real-time GPS and GLONASS precise orbit and clock service [C]//Proceedings of ION GNSS. Savannah, Georgia, 2009: 1885−1891.

[7] LI X, ZHANG X, GUO F. Study on precise point positioning based on combined GPS and GLONASS [C]//Proceedings of ION GNSS, Savannah, Georgia, 2009: 2449−2459.

[8] CAI C, GAO Y. Modeling and assessment of combined GPS/GLONASS precise point positioning [J]. GPS Solutions, 2013, 17(2): 223−236.

[9] MELGARD T, VIGEN E, ØRPEN O. Advantages of combined GPS and GLONASS PPP-experiences based on G2, a new service from Fugro [C]//13th IAIN World Congress. Stockholm, 2009: 1−7.

[10] AXELRAD P, BROWN R G. GPS navigation algorithms [M]// PARKINSON B W, SPILKER J J. Progress in Astronautics and Aeronautics. American: Institute of Astronautics and Aeronautics, 1996: 409−433.

[11] BROWN R G, HWANG P Y. Introduction to random signals and applied Kalman filtering [M]. 3rd ed. New York: Wiley, 1997.

[12] DODSON A H, SHARDLOW P J, HUBBARD L C M, ELGERED G, JARLEMARK P O J. Wet tropospheric effects on precise relative GPS height determination [J]. Journal of Geodesy, 1996, 70(4): 188−202.

[13] GAO Y. P3 user manual (version 1.0) [EB/OL] [2004]. http//people.ucalgary.ca/~ygao/images/P3%20manual.pdf.

[14] SCHMID R. Upcoming switch to IGS08/igs08.atx details on igs08.atx. [IGSMAIL-6355] [EB/OL]. March 7, 2011.

[15] CAI C, GAO Y. Estimation of GPS/GLONASS system time difference with application to PPP [C]//Proceedings of ION GNSS. Savannah, Georgia, 2008: 2880−2887.

一种改进的 GPS/GLONASS 组合精密单点定位算法在露天矿区测量中的应用

蔡昌盛，罗小敏，朱建军

中南大学 地球科学与信息物理学院，长沙 410083

摘　要：提出一种改进的组合 GPS/GLONASS 精密单点定位（GG-PPP）算法，即首先利用传统的 GG-PPP 算法求得 GPS-GLONASS 系统时间差参数和天顶对流层延迟参数，然后将它们作为改进 GG-PPP 算法解算的先验信息，从而达到减少待估参数个数的目的。采用 BJFS 站的实测数据在一个模拟的露天矿区环境进行改进的 GG-PPP 算法试验。结果表明，在有限的卫星可视环境中，改进的 GG-PPP 算法能有效改善定位性能。

关键词：GPS；GLONASS；精密单点定位；卫星高度角；露天矿区

(Edited by Sai-qian YUAN)